Eur. Phys. J. C (2025) 85:989
https://doi.org/10.1140/epjc/s10052-025-14726-5

THE EUROPEAN PHYSICAL JOURNAL C

Regular Article - Theoretical Physics

# Charged regular black holes in quantum gravity: from thermodynamic stability to observational phenomena

**Erdem Sucu**[a], **İzzet Sakallı**[b]

Physics Department, Eastern Mediterranean University, via Mersin 10, 99628 Famagusta, North Cyprus, Turkey

Received: 4 March 2025 / Accepted: 3 September 2025


**Abstract** We investigate the thermodynamic, astrophysical, and observational properties of charged nonsingular black holes within the framework of quantum gravity and nonlinear electrodynamics. Our study focuses on the Frolov black hole model, which generalizes the Reissner–Nordström and Hayward solutions through the inclusion of a cosmological-type parameter $\alpha$. By employing the Gauss–Bonnet theorem (GBT), we derive the Hawking temperature and heat capacity, identifying phase transition points that govern black hole stability. We extend this analysis by incorporating generalized uncertainty principle corrections, revealing modifications to entropy and thermodynamic behavior. In the context of weak gravitational lensing, we compute the deflection angle using GBT and analyze its variations in vacuum and plasma media, emphasizing the role of charge and quantum effects on light propagation. Furthermore, we examine quasi-periodic oscillations by evaluating epicyclic frequencies in accretion disks, linking them to astrophysical observables. Lastly, we study the gravitational time delay of light signals, demonstrating how quantum-modified spacetime alters light propagation. Our results provide key insights into quantum-gravitational corrections to black hole physics, offering potential observational signatures relevant to gravitational wave studies, black hole imaging, and precision tests of strong-field gravity. Throughout this work, the term quantum gravity is used in an effective sense, referring to quantum aspects of black hole physics such as GUP-induced corrections, rather than to a complete and established quantum theory of gravitation.

## 1 Introduction

Black holes have long fascinated physicists due to their role as natural laboratories where general relativity, quantum mechanics, and thermodynamics converge [1–5]. These enigmatic objects not only deepen our understanding of gravitational physics but also provide insights into high-energy astrophysical phenomena [6–8]. Among various black hole models, nonsingular (NS) or regular black holes have gained attention as they offer a resolution to singularity issues inherent in classical solutions. One particularly compelling example is the Frolov black hole [9], a charged NS black hole that generalizes well-known solutions such as the Schwarzschild [10], Reissner–Nordström [11], and Hayward models [12]. This model serves as a crucial platform for investigating quantum-gravitational modifications and their impact on black hole physics. Another notable class of such NS black hole solutions arises from nonlinear electrodynamics (NLED), where the presence of a self-interacting electromagnetic field modifies the black hole structure. In particular, the Hayward black hole and magnetically charged solutions based on rational NLED serve as significant examples of how NLED influences the near-horizon geometry and regularity conditions of black holes [13–15].

The presence of charge in NS black hole models introduces unique thermodynamic and dynamic properties [16]. Specifically, the metric function of the Frolov black hole is characterized by the charge parameter $q$ and a cosmological type parameter $\alpha$, which govern the structure and stability of the event horizon [17]. These parameters encapsulate potential quantum-gravitational effects, making them an essential aspect of our study. Our primary objective is to examine how these corrections influence black hole thermodynamics [18–37], gravitational lensing [38–46], quasi-periodic oscillations (QPOs) [47–53], and accretion processes [54,55].

[a] e-mail: erdemsc07@gmail.com

[b] e-mail: izzet.sakalli@emu.edu.tr (corresponding author)

Published online: 15 September 2025

While our approach involves both the extension of gravity through the Frolov nonsingular model and the implementation of GUP, the motivation is to explore their combined interplay to address a fundamental question in black hole physics: how do ultraviolet quantum corrections and infrared geometric modifications jointly influence observable phenomena? The GUP encodes high-energy quantum effects originating from Planck-scale physics [56–58], whereas the Frolov parameter $\alpha$ represents a geometric modification of spacetime that regularizes classical singularities [9]. Studying them together allows us to separate contributions from ultraviolet versus infrared sectors, thereby revealing distinct physical signatures that cannot be obtained from either framework alone. For instance, GUP corrections primarily suppress Hawking temperature peaks and modify entropy scaling [59,60], while the parameter $\alpha$ alters phase transition locations, deflection angles, and time-delay effects [61,62]. This separation of effects provides testable predictions for distinguishing quantum gravity signatures from modified gravity effects in astrophysical observations, thus clarifying the respective physical consequences rather than obscuring the purpose of the work. The combined framework offers a comprehensive approach to understanding how different aspects of beyond-standard-model physics manifest in black hole phenomena, which is essential for interpreting future high-precision observations from gravitational wave detectors and black hole imaging experiments [55,63].

A major component of our analysis focuses on the thermodynamic properties of the Frolov black hole. Black hole thermodynamics plays a fundamental role in gravitational physics, revealing deep connections between entropy, energy, and information theory [1,64]. We employ the GBT [65–71] as a topological tool to determine the Hawking temperature [72] and heat capacity. Additionally, we incorporate the Generalized Uncertainty Principle (GUP) [73–81] to account for quantum corrections, leading to modified entropy and temperature profiles. These quantum effects provide significant insight into the microscopic nature of black hole entropy [82,83] and the quest for a quantum theory of gravity. Another key aspect of our investigation is gravitational lensing [84], an observational probe of black hole spacetimes. By following the study of Gibbons and Werner [65] , we derive the weak deflection angle [85–87] of light rays around the Frolov black hole via the GBT. We further extend this analysis by considering the influence of a plasma medium, which alters the refractive index of spacetime, thereby affecting the observed deflection angle. Understanding these effects is crucial for astrophysical observations and for differentiating between classical and modified black hole solutions.

In addition, we study QPOs, which serve as important observational signatures of black holes. These oscillations arise from the motion of particles in accretion disks and provide valuable constraints on the underlying spacetime geometry. By computing the epicyclic frequencies [88] of test particles, we establish a relationship between QPO frequencies and black hole parameters, particularly $q$ and $\alpha$. This analysis not only offers a theoretical framework for interpreting observational data but also contributes to tests of GR in the strong-field regime. We also explore gravitational time delay [89–94], a relativistic effect wherein light experiences a delay while propagating through curved spacetime. By calculating the time delay in the Frolov black hole background, we examine how charge and quantum corrections influence light propagation. Time-delay measurements have historically played a crucial role in validating GR and could be instrumental in distinguishing between classical and quantum-modified black hole models [95]. This analysis enhances our understanding of how modified spacetime geometry affects observable emission profiles. Such studies are relevant to ongoing efforts in black hole imaging, particularly those conducted by the Event Horizon Telescope (EHT) [96], which seeks to resolve black hole shadows [63] and accretion flows at unprecedented resolutions. Our motivation for this study stems from the necessity of bridging classical GR with quantum-gravitational corrections. In this regard, the Frolov black hole provides a well-suited model for investigating how charge, quantum effects, and modified gravity influence black hole behavior. By addressing fundamental questions in black hole physics, we aim to contribute to understanding of gravity and its possible extensions beyond Einstein's theory. Moreover, throughout this study, we emphasize that our use of the term "quantum gravity" refers to effective quantum corrections and phenomenological modifications inspired by various approaches to quantum gravity, rather than a complete quantum theory of gravitation. Our framework incorporates well-established quantum field theory effects in curved spacetime and GUP-motivated corrections that capture expected features of a future quantum gravity theory, while remaining within the realm of semiclassical physics [97,98].

This paper is structured as follows: In Sect. 2, we revisit the dynamics of the charged NS black hole framework, focusing on its metric properties and event horizon structure. We discuss how the parameters $q$ (electric charge) and $\alpha$ (cosmological parameter) govern the black hole's horizon topology and influence gravitational interactions. Section 3 explores the thermodynamic properties of NS black holes using GBT. We derive the Hawking temperature and heat capacity, providing insight into the thermodynamic stability. Additionally, we incorporate quantum gravitational corrections via the GUP to modify entropy and temperature. In Sect. 4, we analyze the Hawking temperature of NS black holes with GUP effects, incorporating quantum corrections to examine their impact on black hole thermodynamics. In Sect. 5 applies the GBT to compute the weak deflection angle. Section 6 investigates the weak deflection angle of light in the plasma medium, demon-

strating how variations in the refractive index influence gravitational lensing. Section 7 explores the QPOs around charged NS black holes, analyzing the impact of radial distance on the test particle's angular velocity. In Sect. 8, we examine the gravitational time delay of light signals in NS black hole spacetime. By solving the null geodesic equations, we determine the time delay for light propagating from a source to an observer, incorporating charge and cosmological corrections. Finally, in Sect. 9, we summarize our findings and discuss their broader implications for black hole physics, astrophysics, and quantum gravity. We also outline future directions for extending this study, particularly in the context of multi-messenger astrophysics and observational tests of modified gravity theories.

## 2 Revisiting the dynamics of NS black hole framework

The NS black hole is an extension of the Hayward black hole, incorporating electric charge as an extra parameter, as detailed in [9]. Its spacetime metric is given by:

$$ds^2 = -f(r)dt^2 + \frac{1}{f(r)}dr^2 + r^2 d\Omega^2, \tag{1}$$

where $d\Omega^2 = d\theta^2 + \sin^2\theta d\phi^2$and metric function $f(r)$ is explicitly given by:

$$f(r) = 1 - \frac{r^2(2Mr - q^2)}{r^4 + (2Mr + q^2)\alpha^2}. \tag{2}$$

Here, $M$ represents the black hole mass, while $\alpha$ corresponds to the Hubble length that governs the effective cosmological constant $\Lambda = 3/\alpha^2$. The choice of the Hubble length $\alpha$ as a governing scale is motivated by Frolov's construction of nonsingular black holes [9], where $\alpha$ acts as a cosmological-type parameter that reflects the large-scale structure of spacetime. Physically, $\alpha$ encapsulates the contribution of quantum vacuum energy and provides an effective cosmological constant within the black hole interior, representing infrared modifications to the spacetime geometry. This connection emerges from quantum gravity considerations where the vacuum energy density creates a repulsive effect that regularizes the central singularity [12,99]. The parameter $\alpha$ thus bridges microscopic quantum effects with macroscopic gravitational phenomena, making the metric function (2) not merely phenomenological but connected to the broader program of regular black hole models that resolve classical singularities through quantum-gravitational corrections [61,100]. This approach is consistent with other nonsingular black hole constructions where a fundamental length scale, often associated with quantum gravity effects, regularizes the spacetime curvature at small radii [101,102]. This parameter contributes a "universal hair" to the black hole, bounded by the inequality [16]:

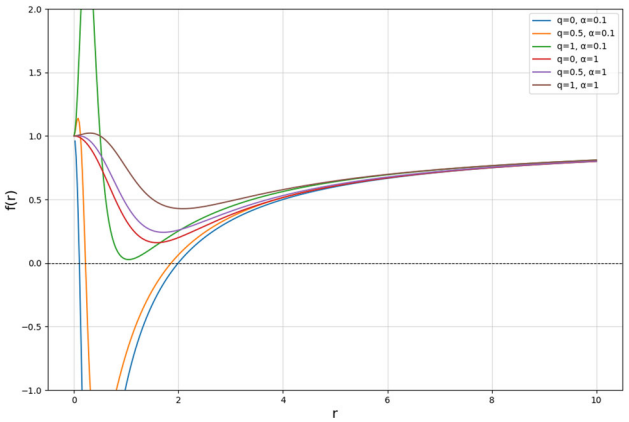


**Fig. 1** Plot of $f(r)$ versus the horizon radius for different values of $\alpha$ and $q$. Here, $M$ is set to 1

$$\alpha \leq \frac{27M}{16}. \tag{3}$$

Such constraints emphasize the critical role of quantum gravity in influencing the black hole structure. Throughout this section, we normalize $M = 1$ for simplicity. Furthermore, the electric charge $q$ characterizes an additional "specific hair" with the constraint $0 \leq q \leq 1$. In specific limits, this model recovers established black hole solutions: the Hayward black hole when $q = 0$, the Reissner–Nordström black hole when $\alpha = 0$, and the Schwarzschild black hole when both $q = 0$ and $\alpha = 0$.

Figure 1 illustrates the metric function $f(r)$ for varying parameters $q$ and $\alpha$. When $q = 0$, increasing $\alpha$ transforms the black hole from a Schwarzschild-type to a structure with multiple horizons, eventually leading to a single-horizon configuration or horizonless spacetime as $\alpha$ approaches its upper limit.

### 2.1 Kretschmann scalar and singularity

We calculate the Kretschmann scalar, which measures the spacetime curvature, to further examine the singularities and curvature characteristics of this black hole. The following gives the Kretschmann scalar:

$$K = R_{\mu\nu\rho\sigma} R^{\mu\nu\rho\sigma}, \tag{4}$$

in which the Riemann curvature tensor is denoted by $R_{\mu\nu\rho\sigma}$. The Kretschmann scalar related to the NS black hole (1) can be computed as follows

$$K = \frac{-144M^2\alpha^4q^2}{r^{10}} + \frac{36M^2\alpha^2q^2}{r^8} + \frac{40M^2\alpha^2}{r^6} + \frac{3M^2 + 3q^2}{r^4} - \frac{6M\,q^2}{r^5} - \frac{2M}{r^3}. \tag{5}$$

At $r = 0$, the Kretschmann scalar proves to be divergent, indicating a curvature singularity at the black hole's core.

This result supports the well-established notion that black hole solutions must feature a central singularity where spacetime curvature becomes infinite.

## 3 Hawking temperature and heat capacity of NS BLACK HOLES via GBT

GBT provides an elegant and topological approach to determining the Hawking temperature of black holes. This method leverages the 2D Euler characteristic in conjunction with the GBT. To outline the process, we consider a general static and spherically symmetric black hole, whose spacetime geometry can be described by a 4D metric like Eq. (1). Through a Wick rotation ($\tau = it$) and a fixation $\theta = \pi/2$, this metric reduces to a 2D Euclidean Schwarzschild-like form:

$$ds^2 = f(r)d\tau^2 + \frac{1}{f(r)}dr^2. \tag{6}$$

The Ricci scalar $R$ for this 2D metric is obtained as:

$$R = -\frac{d^2 f(r)}{dr^2}. \tag{7}$$

By employing the GBT, the expression for the Hawking temperature of 2D black holes is obtained as [69,72]:

$$T_H = \frac{\hbar c}{4\pi \chi k_B} \sum_{j \leq \chi} \int_{r_{hj}} \sqrt{g} R dr, \tag{8}$$

in which $\hbar$ is the reduced Planck constant, $c$ is the speed of light, $k_B$ denotes the Boltzmann constant, $R$ is the Ricci scalar, $g$ is the determinant of the 2D Euclidean metric, $r_{hj}$ identifies the $j$-th Killing horizon, and $\chi$ represents the Euler characteristic of the manifold.

In the context of a Frolov black hole, the Hawking temperature (8) is expressed, in natural units, as follows:

$$T_H = \frac{-Mr_h^6 + q^2 r_h^5 + 4M^2 r_h^3 \alpha^2 + 2Mq^2 r_h^2 \alpha^2 - q^4 r_h \alpha^2}{2\pi \left(r_h^4 + (2Mr_h + q^2)\alpha^2\right)^2}. \tag{9}$$

With distinct curves that signify different values of the Hubble parameter $\alpha$, Fig. 2 shows the relationship between the variables $T_h$ and $r_h$. $T_h$ first rises to a maximum point before falling as $r_h$ increases. This suggests that the two variables have a complicated relationship that is impacted by the parameter $\alpha$. The value of $\alpha$ determines the precise form of the curves and the location of the maximum point. This implies that $\alpha$ has a major influence on how the system behaves as a whole.

The Hawking–Bekenstein entropy is famously defined by [103] as

$$S = \pi r_h^2. \tag{10}$$

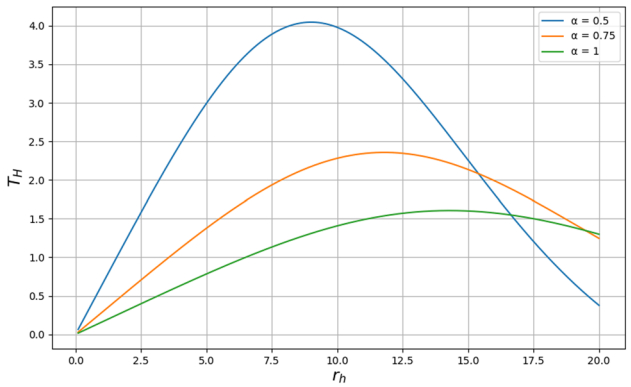


**Fig. 2** Plot of $T_H$ versus the horizon radius for different values of $\alpha$ and q. Here, $M = 10{,}000$ and $q$ is set to 1

To provide a comprehensive thermodynamic analysis, the heat capacity of the black hole system is derived as follows:

$$C = T_H \frac{\partial S}{\partial T_H}. \tag{11}$$

Whence, the explicit expression for $C$ can be found as

$$C = \frac{\Delta}{\Sigma}, \tag{12}$$

in which

$$\Delta = 2\pi r_h^2 \big(8M^3\alpha^4 r_h^3 + 8M^2\alpha^4 q^2 r_h^2 + 2M^2\alpha^2 r_h^6 + 3M\alpha^2 q^2 r_h^5 - Mr_h^9 - \alpha^4 q^6 + q^2 r_h^8\big), \tag{13}$$

and

$$\Sigma = 8M^3\alpha^4 r_h^3 + 12M^2\alpha^4 q^2 r_h^2 - 28M^2\alpha^2 r_h^6 + 6M\alpha^4 q^4 r_h - 12M\alpha^2 q^2 r_h^5 + 2Mr_h^9 - \alpha^4 q^6 + 12\alpha^2 q^4 r_h^4 - 3q^2 r_h^8. \tag{14}$$

In Fig. 3 for varying values of the Hubble length parameter $\alpha$, the graphic shows the heat capacity $C$ as a function of the horizon radius $r_h$, exposing phase transitions through its divergences. Since these divergences correlate to locations where the heat capacity becomes infinite, signifying a shift in thermodynamic stability, they imply second-order phase transitions. Stable configurations are shown by positive $C$ regions, while unstable configurations are indicated by negative $C$ regions. The locations of these phase-transition sites change with $\alpha$, demonstrating how the coupling parameter affects the thermodynamic behavior of the system.

## 4 HAWKING temperature of NS black holes with GUP effect

GUP, an extension of Heisenberg's uncertainty concept, integrates the effects of quantum gravity and posits a basic minimum length scale. This modification revises the traditional

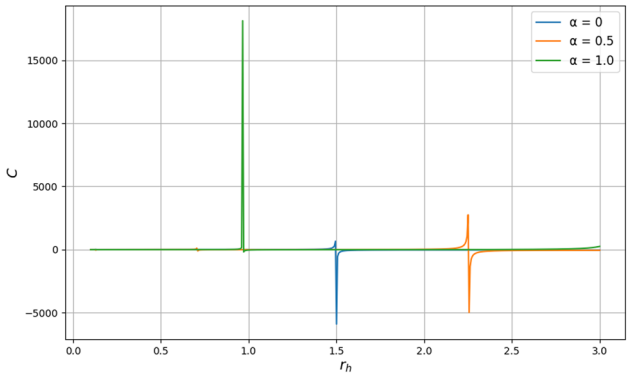


**Fig. 3** The relationship between $C$ and the horizon radius for different values of $\alpha$: $M$ and $q$ are set to 1

uncertainty principles for position and momentum [104]. Such GUP-based modifications have been thoroughly investigated in black hole thermodynamics, proving their impact on entropy and other properties in charged or rotating black hole topologies.

Subsequently, we investigate the influence of GUP modifications on the thermal profile of an NS black hole. This involves using the metric provided in (1) within the modified Klein–Gordon equation (15), associated with a scalar field affected by GUP corrections [74].

$$-(i\hbar)^2\partial^t\partial_t\Psi = \left[(i\hbar)^2\partial^i\partial_i + m_p^2\right] \times \left[1 - 2\beta_{GUP}(i\hbar)^2\partial^i\partial_i + m_p^2\right]\Psi, \tag{15}$$

where $m_p$ denotes the mass of the particle being studied and $\beta_{GUP}$ quantifies the magnitude of the GUP effects. To employ the Wentzel–Kramers–Brillouin (WKB) approximation [105], one can choose

$$\Psi(t, r, \theta, \psi) = \exp\left(\frac{i}{\hbar}S(t, r, \theta, \psi)\right), \tag{16}$$

where $S(t, r, \theta, \psi)$ denotes the tunneling action. Using the Hamilton–Jacobi approach [74], the action is simplified to:

$$S(t, r, \theta, \psi) = -\epsilon t + W(r) + j\psi + c, \tag{17}$$

where $E$ and $j$ represent the energy and angular momentum of the particle. In accordance with [106,107], the particle tunneling probability for escape from black hole is:

$$\Gamma \approx \exp(-4\,\mathrm{Im}W(r_h)) = \exp\left(\frac{\epsilon}{T_{GUP}}\right). \tag{18}$$

Although the WKB-based tunneling method has been widely applied in black hole thermodynamics [108,109], our novelty lies in applying it to the Frolov nonsingular black hole where the interplay of the cosmological-type parameter $\alpha$ and GUP corrections leads to qualitatively distinct thermodynamic behavior. In particular, the simultaneous presence of both modifications creates unique signatures: the shift of critical radii due to geometric regularization effects, the suppression of Hawking temperature peaks through quantum corrections, and the modification of phase transition structures that cannot be obtained from standard general relativistic black holes [60,110]. This combined framework allows us to separate the contributions of infrared geometric modifications (through $\alpha$) from ultraviolet quantum effects (through $\beta_{GUP}$), providing distinct observational signatures for testing different aspects of quantum gravity theories. The resulting temperature profiles and stability conditions offer new insights into how nonsingular spacetime geometry and quantum corrections jointly influence black hole evaporation processes [56]. By substituting the findings into the modified Klein–Gordon equation, we solve for $W(r)$ and get these results: Although the WKB-based tunneling method has been widely applied in black hole thermodynamics [108,109], our novelty lies in applying it to the Frolov nonsingular black hole where the interplay of the cosmological-type parameter $\alpha$ and GUP corrections leads to qualitatively distinct thermodynamic behavior. In particular, the simultaneous presence of both modifications creates unique signatures: the shift of critical radii due to geometric regularization effects, the suppression of Hawking temperature peaks through quantum corrections, and the modification of phase transition structures that cannot be obtained from standard general relativistic black holes [60,110]. This combined framework allows us to separate the contributions of infrared geometric modifications (through $\alpha$) from ultraviolet quantum effects (through $\beta_{GUP}$), providing distinct observational signatures for testing different aspects of quantum gravity theories. The resulting temperature profiles and stability conditions offer new insights into how nonsingular spacetime geometry and quantum corrections jointly influence black hole evaporation processes [56].

$$W(r_h) = \frac{i\pi\epsilon}{f'(r_h)\sqrt{1 - 2\beta_{GUP}m_p^2}}, \tag{19}$$

which results in the GUP-influenced Hawking temperature:

$$T_{GUP} = \frac{f'(r_h)}{4\pi}\sqrt{1 - 2m_p^2\beta_{GUP}}. \tag{20}$$

The specific square-root form of the correction in Eq. (20) arises naturally in several well-established approaches to quantum gravity, rather than being an ad hoc phenomenological choice. In string theory, the fundamental string length $l_s$ introduces a minimal length scale that modifies the canonical commutation relations, leading to corrections of the form $\sqrt{1 - \beta l_p^2 p^2}$ in the energy–momentum dispersion relation [111,112]. Similarly, in loop quantum gravity, the discrete structure of spacetime at the Planck scale generates analogous modifications through the polymer quantization procedure [113,114]. Doubly special relativity frameworks, which

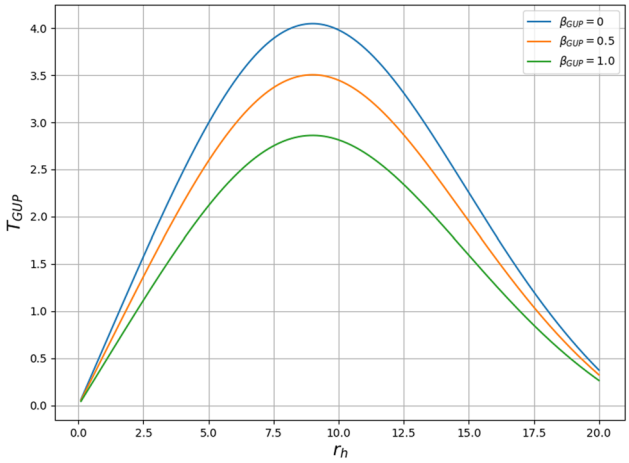


**Fig. 4** This graph illustrates the relationship between GUP temperature and event horizon, varying with $\beta_{GUP}$. Parameters are set as follows: $M = 10{,}000$, $q = 1$, and $\alpha = m_p = 0.5$

incorporate both a maximal energy (Planck energy) and minimal length (Planck length), also yield square-root corrections to thermodynamic quantities [115,116]. These diverse approaches converge on the same functional form because they all implement a fundamental length scale that regularizes ultraviolet divergences through modified phase space geometry. Thus, the phenomenological expression employed here represents a universal low-energy manifestation of these fundamental models, reflecting the common feature that quantum gravity effects introduce a minimal length scale that modifies the standard uncertainty principle [117,118]. The universality of this correction across different quantum gravity approaches provides strong theoretical justification for its application to black hole thermodynamics.

In the limit of $\beta_{GUP} \to 0$, the equation reduces to the classical Hawking temperature (9). Figure 4 demonstrates that for larger black hole masses, GUP modifications become significant, causing a temperature decrease. In fact, Fig. 4 depicts the influence of quantum gravity by plotting the Hawking temperature modification $T_{GUP}$ against the event horizon $r_h$ for different values of the GUP parameters $\beta_{GUP}$. Increasing $\beta_{GUP}$ lowers and shifts the temperature peak to a smaller $r_h$, as $T_{GUP}$ initially rises to a peak before dropping with larger $r_h$. $\beta_{GUP} = 0$ corresponds to the classical Hawking temperature, while greater $\beta_{GUP}$ diminishes thermal intensity and temperature peaks, highlighting the GUP's influence on black hole thermodynamics.

Furthermore, we analyze the effect of the GUP modification on the entropy and heat capacity of the NS black hole. As per the standard black hole thermodynamics, the entropy is given by Eq. (10). Using the corrected Hawking temperature $T_{GUP}$ from Eq. (20), the heat capacity at constant charge is derived as:

$$C_q = T_{GUP}\frac{\partial S}{\partial T_{GUP}}. \tag{21}$$

This expression indicates that the introduction of the GUP correction reduces the overall heat capacity, affecting the thermodynamic stability of the black hole. Notably, as $\beta_{GUP}$ increases, the heat capacity decreases, revealing the profound impact of quantum gravitational effects on black hole thermodynamics. Figure 5 illustrates the variation of $C_q$ with respect to $r_h$ for different values of $\beta_{GUP}$, showing that quantum gravity effects influence the black hole's thermal behavior by modifying its stability conditions.

## 5 Weak deflection angle of charged NS black hole via GBT

This section examines the deflection angle in the NS black hole with the GBT using an optical metric, as introduced by Gibbons and Werner formalism [65]. We emphasize that our application follows directly from the foundational work of Gibbons and Werner [65], where the global topological nature of lensing emerges from the Euler characteristic through the Gauss–Bonnet theorem. Their seminal approach established that gravitational deflection can be understood as a topological phenomenon, with the global nature arising from contour integration in the asymptotic region that captures the essential geometric properties of the spacetime [119,120]. While their framework provides the general theoretical foundation, our analysis extends this established method to the Frolov model with charge and Hubble length corrections, thus highlighting how these specific modifications alter the asymptotic contributions and provide new insights into realistic astrophysical scenarios involving nonsingular black holes. The topological insight remains universal, but the specific geometric contributions reveal distinct signatures of quantum-corrected spacetimes [9].

For null geodesics, where $ds^2 = 0$, the metric in Eq. (1) simplifies to:

$$dt^2 = \gamma_{ij}dx^i dx^j = \frac{1}{f^2}dr^2 + \frac{r^2}{f}(d\theta^2 + \sin^2\theta d\phi^2), \tag{22}$$

where $i, j \in \{1, 2, 3\}$ and $\gamma_{ij}$ is the optical metric. By imposing the condition $\theta = \pi/2$, the motion is effectively confined to the $(r, \phi)$ plane.

The Ricci scalar assesses the Gaussian curvature $K$ of the optical metric within this plane:

$$K = \frac{R}{2} = \frac{-144M^2\alpha^4q^2}{r^{10}} + \frac{36M^2\alpha^2q^2}{r^8} + \frac{40M^2\alpha^2}{r^6} + \frac{3M^2 + 3q^2}{r^4} - \frac{6M\,q^2}{r^5} - \frac{2M}{r^3}. \tag{23}$$

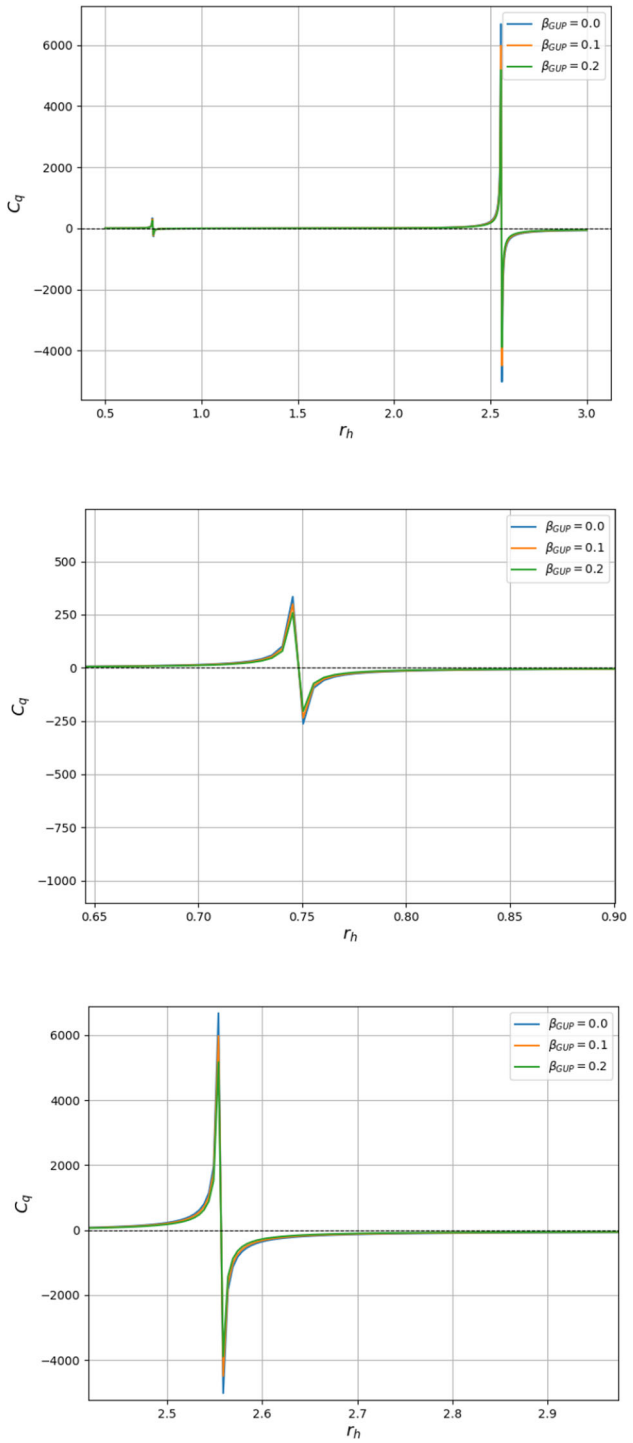


**Fig. 5** Heat capacity $C_q$ is related to the event horizon radius $r_h$ for various values of the GUP parameter $\beta_{GUP}$. The parameters are fixed at $M = 1$, $q = 0.5$, $\alpha = 1$, and $m_p = 1$. The plot shows that an increase in $\beta_{GUP}$ lowers the heat capacity, which means that thermal fluctuations are suppressed by the influence of quantum gravity. Also, the existence of $\beta_{GUP}$ modifies the black hole stability condition, thereby changing the critical points at which phase transitions can or cannot take place

GBT is applied by considering a domain $D$ with boundary $\partial D$, Euler characteristic $\chi$, and Riemannian metric $g$ leading to Gaussian curvature $K$. The theorem is stated as:

$$\iint_D K dS + \int_{\partial D} \kappa dt + \sum_i \alpha_i = 2\pi \chi(D). \tag{24}$$

Here, $S$ represents the source and $O$ represents the observer, with $D$ being the region bounded by a geodesic $C$ and a boundary $C_1$ perpendicular to $C$ at $S$ and $O$. For such a configuration, the sum of exterior angles $\sum_i \alpha_i = \alpha_S + \alpha_O = \pi$ and the Euler characteristic $\chi(D) = 1$, as $D$ is topologically a 2-disk.

The geodesic curvature $\kappa$ along a path $\gamma$ is defined as $k(\gamma) = |\nabla_{\dot\gamma}\dot\gamma|$. Along $C$, $\kappa = 0$, leaving only $\kappa(C_1)$ to be considered. The radial component of $\kappa(C_1)$ is given by:

$$\kappa(C_1)_r = \dot\gamma^\phi \partial_\phi \dot\gamma^r + \Gamma^r_{\phi\phi}\dot\gamma^\phi\dot\gamma^\phi. \tag{25}$$

Over cosmological distances, where $\gamma \sim r =$ constant, the first term vanishes, and the second term evaluates to $\frac{1}{r}$. By substituting $dt \to r d\phi$, the boundary integral becomes the sum of the exterior angles plus the deflection angle $\delta\bar\alpha$:

$$\delta\bar\alpha = -\iint_D K dS. \tag{26}$$

Using the weak deflection limit, the integration bounds are $r : b/\sin\phi < r < \infty$ and $\phi : 0 < \phi < \pi$, where $b$ denotes the impact parameter. Evaluating the integral yields:

$$\delta\bar\alpha = -\frac{3q^2\pi}{4b^2} + \frac{4M}{b} - \frac{4Mq^2}{3b^3} + \frac{315M^2\alpha^4q^2\pi}{64b^8} - \frac{15M^2\alpha^2\pi}{4b^4} - \frac{15M^2\alpha^2q^2\pi}{8b^6} + \frac{3M^2\pi}{4b^2} + \frac{27M^2q^2\pi}{16b^4}. \tag{27}$$

The resulting expression for the deflection angle shows how it varies with charge, mass, and the Hubble parameter $\alpha$. Large values of $\alpha$ significantly increase the lensing angle, indicating modified shooting effects.

The deflection angle $\delta\tilde\alpha$ is plotted against the impact parameter $b$ over a range of values of the Hubble parameter $\alpha$ in Fig. 6. The effects of gravitational lensing become weaker with increased impact parameters, which is consistent with the behavior of weaker gravitational fields farther from the source, since the deflection angle decreases monotonically as $b$ increases. Stronger coupling parameter-induced alterations in gravitational lensing are implied by the deflection angle being substantially improved for smaller $b$ for bigger $\alpha$. At greater impact parameters, the influence of $\alpha$ appears to decrease, since the curves for all $\delta\bar\alpha$ values converge as $b$ increases. In the strong-field regime, this behavior emphasizes how important $\alpha$ is to alter lensing phenomena.

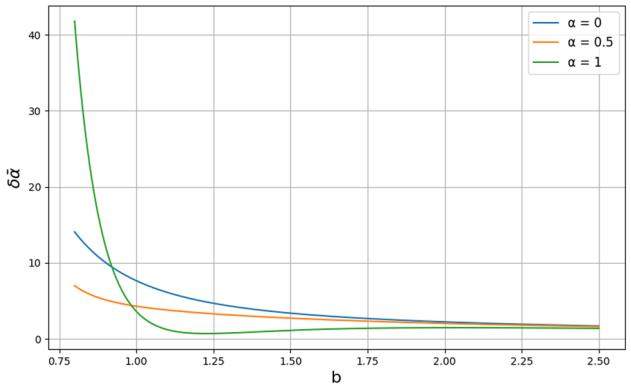


**Fig. 6** Variation of $\delta\bar{\alpha}$ with $b$ for different $\alpha$ values. The graph highlights how changes in $\alpha$ influence the behavior of $\delta\bar{\alpha}$, revealing distinct patterns for each $\alpha$. Here, $M$=1 and $q$ is set to 0.9

## 6 Weak deflection angle in the plasma medium

In this section, we analyze the influence of the plasma medium on weak gravitational lensing for the NS black hole. The refractive index corresponding to this NS black hole is given as:

$$n(r) = \sqrt{1 - \frac{\omega_e^2}{\omega_\infty^2}}, \tag{28}$$

where $\omega_e$ is the plasma frequency of an electron, and $\omega_\infty$ represents the photon frequency as observed at infinity. Consequently, the optical metric is expressed as:

$$d\sigma^2 = n^2(r)\left[f(r)dr^2 + r^2 d\phi^2\right], \tag{29}$$

where the refractive index $n(r)$ is given by [69,121]:

$$n(r) = \sqrt{1 - \frac{\omega_e^2}{\omega_\infty^2} f(r)}. \tag{30}$$

The Gaussian optical curvature can then be evaluated using:

$$K = -\frac{1}{\sqrt{\det \bar{g}}}\left[\frac{\partial}{\partial r}\left(\frac{\sqrt{\det \bar{g}}}{\bar{g}_{rr}}\Gamma^r_{\phi\phi}\right) + \frac{\partial}{\partial \phi}\left(\frac{\sqrt{\det \bar{g}}}{\bar{g}_{\phi\phi}}\Gamma^\phi_{r\phi}\right)\right], \tag{31}$$

where $\bar{g}$ denotes the optical metric. For NS black hole, the Gaussian optical curvature results in

$$\begin{aligned} K \approx & -\frac{3Mw_e^2}{r^{11}w_\infty^2} - \frac{2M}{r^3} + \frac{5q^2w_e^2}{r^4w_\infty^2} + \frac{3}{r^4w_\infty^2} \\ & - \frac{26Mq^2w_e^2}{r^5w_\infty^2} - \frac{6}{r^5w_\infty^2} + \frac{10q^4w_e^2}{w_\infty^2 r^6} + \frac{2q^4}{r^6} \\ & - \frac{23Mq^4w_e^2}{r^7w_\infty^2} - \frac{39\alpha^2q^4w_e^2}{r^8w_\infty^2} + \frac{21\alpha^2q^4}{r^8w_\infty^2} \\ & + \frac{162\alpha^2Mq^4w_e^2}{w_\infty^2 r^9} + \frac{38Mq^4}{r^9} + \frac{171\alpha^4Mq^4w_e^2}{w_\infty^2 r^{11}} \\ & + \frac{90\alpha^4q^4M}{r^{11}}. \end{aligned} \tag{32}$$

For simplicity, we consider the optical curvature up to the first-order terms in $M$ to align with the results obtained in the absence of a plasma medium.

The infinitesimal surface element for the NS black hole is given by

$$ds^2 = \sqrt{\det \bar{g}}\, dr\, d\phi = n(r) r\, dr\, d\phi. \tag{33}$$

To determine the deflection angle in the plasma medium, we apply the GBT. Considering that the light ray starts from infinity and extends to a large distance while remaining nearly straight under weak field approximations, we adopt the straight-line approximation $r = b/\sin\phi$, where $b$ is the impact parameter. The GBT is then formulated as:

$$\bar{\alpha} = -\int\int_{\mathcal{D}_\infty} K\, dS. \tag{34}$$

Under this condition, the deflection angle for the NS black hole becomes:

$$\begin{aligned} \bar{\alpha} = & -\frac{1248\alpha^2q^4\sigma}{35b^7} + \frac{4q^2}{b^3} + \frac{32q^4}{15b^5} - \frac{96\alpha^2q^4}{5b^7} \\ & + \frac{20q^2\sigma}{3b^3} + \frac{32q^4\sigma}{3b^5} + \frac{2835M\alpha^4q^4\pi}{128b^{10}} \\ & - \frac{875M\alpha^2q^4\pi}{128b^8} - \frac{33Mq^2\sigma\pi}{8b^4} + \frac{35Mq^4\sigma\pi}{16b^6} \\ & - \frac{3M\sigma\pi}{2b^2} + \frac{9Mq^2\pi}{8b^4} + \frac{15Mq^4\pi}{8b^6} - \frac{M\pi}{b^2} \\ & + \frac{10773M\alpha^4q^4\sigma\pi}{256b^{10}} + \frac{1575M\alpha^2q^4\sigma\pi}{128b^8}. \end{aligned} \tag{35}$$

where $\sigma = \frac{w_e^2}{w_\infty^2}$. The aforementioned outcome demonstrates that light rays are traveling through the plasma medium. This angle is going to be the non-plasma medium ($\sigma$ goes to zero) if the plasma effects are eliminated.

The graph in Fig. 7 shows how the deflection angle $\bar{\alpha}$, the impact parameter $b$, and the plasma parameter $\sigma$ relate to each other in a specific physical system. For all values of the plasma parameter $\sigma$, the deflection angle $\bar{\alpha}$ decreases as the impact parameter $b$ rises from 1.0 to 1.5. This inverse connection implies that the resulting deflection lessens with increasing distance of closest approach between two interacting particles. Additionally, the graph shows that a drop in the deflection angle occurs when the plasma parameter is increased for a certain value of the impact parameter. This suggests that smaller deflections are produced by a weaker particle-to-particle interaction, which is correlated with a higher plasma parameter. The curves for various values of $\sigma$ converge as b increases, suggesting that the effect of the plasma parameter on the deflection angle diminishes with large impact parameters. Overall, by showing the interaction between the impact parameter, plasma parameter, and the

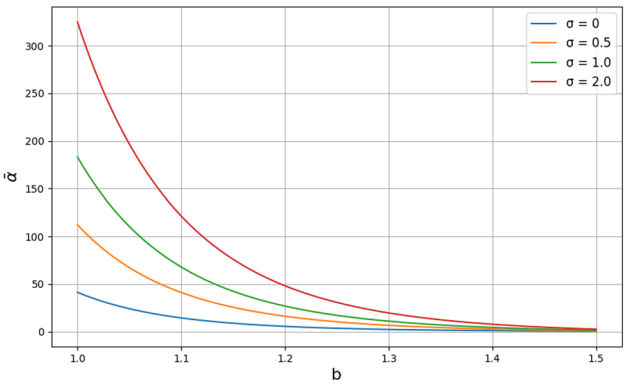


**Fig. 7** Variation of $\bar{\alpha}$ with $b$ for different values of $\sigma$. The plot demonstrates how $\sigma$ influences the behavior of $\bar{\alpha}$ as a function of $b$, highlighting distinct trends for each $\sigma$ value. Here, $M$, $q$ and $\alpha$ are set to 1

consequent deflection angle, this graph might offer insightful information about the scattering process in a plasma environment.

## 7 QPOs around charged NS black holes

QPOs are characterized by frequencies that are not perfectly periodic, but exhibit near-constant behavior. These phenomena are predominantly observed in astrophysical systems such as accretion disks surrounding black holes, neutron stars, and other compact objects under strong gravitational influence.

The oscillatory behavior of QPOs is intricately linked to the fundamental or epicyclic frequencies of test particles in circular orbits within the accretion disk. To calculate these frequencies, the dynamics of a test particle are modeled using the following Lagrangian:

$$L = \frac{1}{2} m g_{\mu\nu} \dot{x}^{\mu} \dot{x}^{\nu}, \tag{36}$$

where $m$ represents the mass of the particle, $x^{\mu}$ its four coordinates, and $\dot{x}^{\mu} = \frac{dx^{\mu}}{d\tau}$ are the components of the four-velocity. The metric components $g_{\mu\nu}$ are functions of the geometry of spacetime. Since the spacetime under consideration is static and spherically symmetric, conserved quantities such as the energy $E = -g_{tt}\dot{t}$ and angular momentum $L = g_{\phi\phi}\dot{\phi}$ arise from the associated Killing vectors. Furthermore, the normalization condition $g_{\mu\nu}\dot{x}^{\mu}\dot{x}^{\nu} = -1$ governs the motion of massive test particles.

From the above, the radial component of the four-velocity satisfies the equation:

$$\frac{1}{f(r)}\dot{r}^2 + r^2\dot{\theta}^2 = V_{\text{eff}}, \tag{37}$$

where the effective potential $V_{\text{eff}}$ is expressed as:

$$V_{\text{eff}} = -1 - \frac{E^2 g_{\phi\phi} + L^2 f(r)}{f(r) g_{\phi\phi}}. \tag{38}$$

For particles in circular orbits within the equatorial plane ($\dot{r} = \dot{\theta} = 0$), the orbital parameters are determined by the following equations:

- The angular velocity of a test particle in a stable circular orbit is given by:

$$\Omega_{\phi} = \sqrt{\frac{-\partial_r g_{tt}}{\partial_r g_{\phi\phi}}} = \sqrt{\frac{f'(r)}{2r}}. \tag{39}$$

  This quantity describes the rate at which a test particle moves around the black hole in terms of coordinate time $t$.
- The time component of the four-velocity, denoted as $u^t = \dot{t}$, is:

$$\dot{t} = u^t = \frac{1}{\sqrt{-g_{tt} - g_{\phi\phi}\Omega_{\phi}^2}} = \frac{1}{\sqrt{f(r) - \frac{rf'(r)}{2}}}. \tag{40}$$

  This describes how the coordinate time $t$ evolves with respect to the proper time $\tau$ of the particle.
- The conserved energy of a test particle (per unit mass) in a circular orbit is:

$$E = \frac{-g_{tt}}{\sqrt{-g_{tt} - g_{\phi\phi}\Omega_{\phi}^2}} = \frac{f(r)}{\sqrt{f(r) - \frac{rf'(r)}{2}}}. \tag{41}$$

  This represents the total energy of the particle due to its motion in the gravitational field.
- The conserved angular momentum of the test particle (per unit mass) is:

$$L = \frac{g_{\phi\phi}\Omega_{\phi}}{\sqrt{-g_{tt} - g_{\phi\phi}\Omega_{\phi}^2}} = \frac{r\sqrt{\frac{rf'(r)}{2}}}{\sqrt{f(r) - \frac{rf'(r)}{2}}}. \tag{42}$$

  This represents the orbital angular momentum of the particle, which is conserved in the absence of external torques.

### 7.1 The small oscillations approximation

In the regime of small perturbations around equilibrium, radial and angular displacements are denoted as $r \approx r_0 + \delta r$ and $\theta \approx \pi/2 + \delta\theta$. The perturbative equations take the form:

$$\frac{d^2\delta r}{dt^2} + \Omega_r^2 \delta r = 0, \quad \frac{d^2\delta\theta}{dt^2} + \Omega_{\theta}^2 \delta\theta = 0, \tag{43}$$

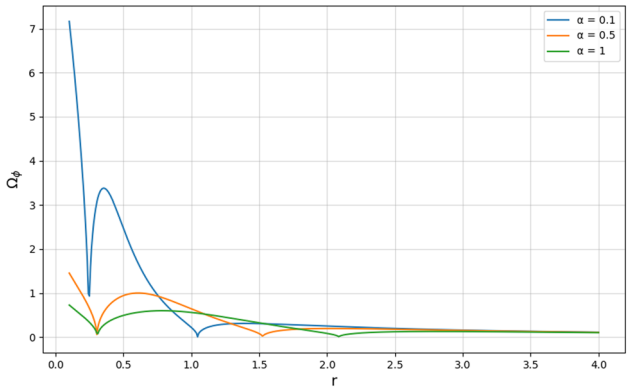


**Fig. 8** Plots of angular frequency as a function of $r$ for different values of $\alpha$, with fixed parameters $M = 1$ and $q = 1$

where the epicyclic frequencies $\Omega_r$ and $\Omega_\theta$ are derived as [122,123]:

$$\Omega_r^2 = -\frac{1}{2g_{rr}(u^t)^2}\left.\frac{\partial^2 V_{\text{eff}}}{\partial r^2}\right|_{\theta=\pi/2}, \tag{44}$$

$$\Omega_\theta^2 = -\frac{1}{2g_{\theta\theta}(u^t)^2}\left.\frac{\partial^2 V_{\text{eff}}}{\partial \theta^2}\right|_{\theta=\pi/2}. \tag{45}$$

From these frequencies, the Keplerian frequency is defined as $f_\phi = \Omega_\phi/(2\pi)$ and the radial epicyclic frequency becomes $f_r = \Omega_r/(2\pi)$. Within the relativistic precession model, the lower QPO frequency $f_L$ is associated with periastron precession $f_L = f_\phi - f_r$, while the upper QPO frequency $f_U$ corresponds to the Keplerian frequency $f_U = f_\phi$ [122].

Figure 8 illustrates the dependence of the test particle's angular velocity $\Omega_\phi$ on radial distance $r$ for coupling constants $\alpha = 0.1, 0.5$, and 1. In each scenario, $\Omega_\phi$ starts high at small $r$ and declines, approaching zero with increasing $r$. Smaller $\alpha$ leads to pronounced peaks and greater oscillations in angular velocity, while larger $\alpha$ results in a smoother response with reduced peak values, indicating a stabilizing effect on particle movement. The graph exhibits multiple local extrema, indicating unstable regions in the angular velocity profile. This analysis is pertinent to studying test particle orbits in astrophysical settings such as near black holes or compact stars, where $\alpha$ could represent gravitational correction terms or influences from other fields.

## 8 Gravitational time delay of light in charged NS black holes

This section outlines the theoretical basis for analyzing the time delay of light traveling through a gravitational field. The time delay is determined by solving the null geodesic equations, an approach extensively validated through numerous observations over decades [94]. This method is now standard in physics and astronomy for studying phenomena such as gravitational deflection and time-delay effects [124–126].

In a spherically symmetrical spacetime, the metric is denoted by Eq. (1). Key conserved quantities essential for particle motion are:

$$J = r^2\sin^2\theta\frac{d\phi}{d\lambda}, \quad E = f(r)\frac{dt}{d\lambda}, \quad \epsilon = g_{\mu\nu}\frac{dx^\mu}{d\lambda}\frac{dx^\nu}{d\lambda}. \tag{46}$$

Here, $J$ represents the conserved angular momentum, $E$ is the energy, and $\epsilon$ characterizes the nature of the geodesic (null for photons, $\epsilon = 0$).

When considering equatorial motion ($\theta = \pi/2$), the geodesic equation reduces to:

$$\frac{1}{2}\left(\frac{dr}{d\lambda}\right)^2 + \frac{1}{2}f(r)\left(\frac{J^2}{r^2} + \epsilon\right) = \frac{1}{2}E^2. \tag{47}$$

The dynamics are governed by the effective potential $V_{\text{eff}}(r) = \frac{1}{2}f(r)\left(\frac{J^2}{r^2} + \epsilon\right)$, where $b = |J/E|$ represents the impact parameter. For photons where $\epsilon = 0$, the radial velocity's correlation to time is:

$$\frac{dr}{dt} = \pm f(r)\sqrt{1 - \frac{b^2 f(r)}{r^2}}, \tag{48}$$

where the $\pm$ symbols denote inward or outward motion. In gravitational lensing, light originating from a source at $r_S$ passes a turning point $r_0$ before proceeding to an observer at $r_O$. The condition for the turning point is given by

$$\left.\frac{dr}{d\lambda}\right|_{r=r_0} = 0 \implies b^2 = \frac{r_0^2}{f(r_0)}. \tag{49}$$

The total time delay is calculated as:

$$\Delta T = \int_{r_S}^{r_0}\frac{dr}{f(r)\sqrt{1-\frac{b^2 f(r)}{r^2}}} + \int_{r_0}^{r_O}\frac{dr}{f(r)\sqrt{1-\frac{b^2 f(r)}{r^2}}} - \sqrt{r_S^2 - r_0^2} - \sqrt{r_O^2 - r_0^2}. \tag{50}$$

Table 1 illustrates the gravitational time delay ($\Delta T$) of light as influenced by variations in the coupling constant $\alpha$, charge $q$, and the radial position of the source $r_S$, with fixed values for $M$, $r_O$, $r_0$ and $b$. It reveals key trends, increasing $\alpha$ or $q$ amplifies the time delay, reflecting stronger gravitational effects or spacetime curvature modifications, while larger $r_S$ also increases $\Delta T$ due to the longer light path through the gravitational field. Physically, this demonstrates how parameters like charge and coupling constants in modified gravity or dark matter models shape spacetime geometry and influence photon trajectories. The nonlinear relationships, particularly at high $q$ and $\alpha$, suggest complex interdependencies between these parameters and the gravitational field. This

**Table 1** Gravitational time delay $\Delta T$ for different values of the coupling parameter $\alpha$, charge $q$, and source position $r_S$. The observer and turning point are fixed at $r_O = r_0 = 1$, and the mass and impact parameter are also set to one: $b = M = 1$. The results highlight how variations in $\alpha$ and $q$ influence the gravitational time delay experienced by light propagating through the black hole spacetime

| $\alpha$ | $q$ | $r_S$ | $\Delta T$ |
|---|---|---|---|
| 0.1 | 0.5 | 1.5 | 0.032 |
| 0.1 | 0.5 | 1.6 | 0.444 |
| 0.1 | 0.5 | 1.7 | 1.1897 |
| 0.3 | 0.5 | 1.4 | 0.142 |
| 0.3 | 0.5 | 1.5 | 0.528 |
| 0.3 | 0.5 | 1.6 | 1.173 |
| 0.5 | 0.5 | 1.4 | 2.217 |
| 0.5 | 0.5 | 1.5 | 3.52 |
| 0.5 | 0.5 | 1.6 | 6.411 |
| 0.5 | 0.1 | 1.4 | 0.36 |
| 0.5 | 0.1 | 1.5 | 0.757 |
| 0.5 | 0.1 | 1.6 | 1.363 |
| 0.5 | 0.1 | 1.7 | 2.394 |
| 0.5 | 0.3 | 1.4 | 0.698 |
| 0.5 | 0.3 | 1.5 | 1.241 |
| 0.5 | 0.3 | 1.6 | 2.098 |
| 0.5 | 0.3 | 1.7 | 3.757 |

complexity makes the results significant for probing alternative theories of gravity and dark matter effects in contexts of strong gravitational lensing.

## 9 Conclusion

In this study, we investigated the properties of a charged NS black hole within the framework of quantum gravity and NLED. Our primary goal was to analyze the modifications introduced by these corrections on black hole thermodynamics, gravitational lensing, and astrophysical observables such as QPOs and time-delay effects. The metric under consideration, given by Eq. (1), incorporates a charge parameter $q$ and a cosmological-type NLED parameter $\alpha$, which significantly influence the event horizon structure and thermodynamic stability of the black hole. By examining these effects in detail, we provided a comprehensive analysis of how such modifications impact both theoretical and observational aspects of black hole physics.

One of the key aspects of our study was the analysis of the thermodynamic properties of the charged NS black hole. Using the GBT, we derived the Hawking temperature, given in Eq. (9), which exhibits a non-trivial dependence on the parameters $q$ and $\alpha$. Our analysis revealed that increasing the charge parameter $q$ generally suppresses the temperature, leading to a prolonged evaporation time. Moreover, the presence of the universal hair parameter $\alpha$ affects the peak temperature and shifts the thermodynamic equilibrium, as demonstrated in Fig. 2. This suggests that quantum gravity effects play a significant role in black hole thermodynamics by introducing deviations from classical predictions. We extended our thermodynamic analysis by incorporating the GUP, which accounts for quantum gravitational corrections. The GUP-modified Hawking temperature, expressed in Eq. (20), highlights how quantum effects suppress the temperature, effectively delaying the evaporation process of the black hole. Figure 4 illustrates this suppression, indicating that stronger GUP corrections lead to lower temperature peaks and enhanced stability of the black hole. Additionally, we computed the heat capacity $C$, given by Eq. (3), and demonstrated that its divergence marks the onset of phase transitions. As shown in Fig. 3, these phase transitions are influenced by both $q$ and $\alpha$, reinforcing the idea that modified gravity plays a crucial role in black hole thermodynamics.

Another essential part of our investigation was the study of gravitational lensing. By employing the GBT in the weak-field approximation, we derived the deflection angle $\delta\bar{\alpha}$ for the charged NS black hole. Our results, presented in Eq. (27), indicate that the deflection angle increases for smaller impact parameters $b$, confirming the influence of black hole charge and quantum corrections. Figure 6 provides a visualization of how the deflection angle varies with $b$ for different values of $\alpha$, demonstrating that increasing $\alpha$ enhances the bending of light rays. Thus, the latter remarks suggest that modified gravity corrections could have observational signatures detectable in future lensing studies. Additionally, we extended our gravitational lensing analysis to include the effects of a plasma medium, which modifies the refractive index of the surrounding spacetime. The modified deflection angle in the presence of plasma, which is given by Eq. (35), exhibits notable deviations compared to the vacuum case. As shown in Fig. 7, the plasma parameter $\sigma$ significantly affects the bending of light, implying that the properties of astrophysical environments must be carefully considered when interpreting gravitational lensing observations.

Furthermore, we examined QPOs around the charged NS black hole by computing the fundamental frequencies associated with particle motion in the accretion disk. Using the radial and epicyclic frequencies derived in Eqs. (44) and (45), we determined the characteristic frequencies governing the QPOs. Figure 8 illustrates the angular frequency $\Omega_\phi$ as a function of the radial coordinate $r$, highlighting the impact of $\alpha$ on the stability and oscillation modes of the accretion of matter. These results provide a potential avenue for testing modified gravity models through X-ray observations of black hole candidates. We also investigated the gravitational time delay effect, which serves as a key observational probe of strong-field gravity. The time delay expression, given by

Eq. (50), quantifies the influence of charge and quantum corrections on photon travel times. The numerical values presented in Table 1 illustrate how varying the parameters $q$ and $\alpha$ affects the observed time delay. Our findings suggest that future high-precision gravitational time-delay measurements could serve as an independent test of quantum-modified black hole models.More broadly, our results provide fundamental insights into the interplay between high-energy quantum effects and gravitational phenomena in black hole physics. The GUP corrections, representing Planck-scale modifications to the uncertainty principle, manifest as suppressed evaporation rates and enhanced thermodynamic stability through reduced heat capacity. This suggests that quantum gravity naturally prevents thermal runaway in black holes, potentially resolving aspects of the information paradox by ensuring the existence of stable black hole remnants [56,127]. The geometric modifications encoded in the parameter $\alpha$ demonstrate how quantum vacuum energy and infrared modifications can fundamentally alter causal structure, phase transitions, and observable signatures such as deflection angles and time delays. The separability of ultraviolet ($\beta_{GUP}$) and infrared ($\alpha$) effects provides a novel framework for distinguishing different quantum gravity scenarios in observational data [128,129]. Together, these effects provide a bridge between Planck-scale physics and astrophysical observations, offering a test bed for the interplay between quantum mechanics and gravitation. The combined framework reveals that high-energy quantum corrections primarily affect thermodynamic stability and evaporation dynamics, while geometric modifications influence causal propagation and lensing phenomena [130,131]. This separation of physical effects enables targeted observational tests: GUP signatures could be detected through precision measurements of black hole evaporation in primordial black holes, while $\alpha$-induced modifications could be observable in gravitational lensing surveys and black hole shadow measurements. The universality of these corrections across different black hole parameters suggests fundamental principles that could guide the development of complete quantum theories of gravity [132–134].

Looking ahead, several promising directions could emerge from our study. One immediate extension would be to explore the strong-field lensing regime [135], where higher-order corrections could yield observationally testable deviations from general relativity [136]. Another study might involve extending our thermodynamic analysis by incorporating alternative quantum gravity models, such as string-inspired modifications [137] or noncommutative geometry effects [138]. Additionally, the study of black hole shadows and their interplay with NLED could provide further insight into the nature of singularity-free black holes. Future work could also investigate how the presence of dark matter halos [139] surrounding black holes influences the observed astrophysical signatures of such modified spacetimes. Finally, the development of numerical simulations that incorporate charged NS black holes in hydrodynamical accretion models [140,141] could enhance our understanding of observational constraints in modified gravity theories.

**Acknowledgements** We express our sincere gratitude to the Editor and anonymous Reviewers for their constructive comments and valuable suggestions that significantly improved the quality and clarity of this manuscript. We also express our gratitude to EMU, TÜBİTAK, ANKOS, and SCOAP3 for their academic support. We also acknowledge COST Actions CA22113, CA21106, and CA23130 for their contributions to networking.

**Funding** The work was carried out without any direct financial support or sponsorship from public, commercial, or not-for-profit funding agencies.

**Data Availability Statement** This manuscript has no associated data. [Author's comment: Data sharing is not applicable to this article as no datasets were generated or analyzed during the current theoretical study.]

**Code Availability Statement** This manuscript has no associated code/software. [Author's comment: Code/Software sharing is not applicable to this article as no code or software was generated or analyzed during the current theoretical study.]


Funded by SCOAP[3].

## References

1. R.M. Wald, The thermodynamics of black holes. Living Rev. Relativ. **4**, 1–44 (2001)
2. P.C.W. Davies, Thermodynamics of black holes. Rep. Prog. Phys. **41**, 1313 (1978)
3. S.W. Hawking, Black holes and thermodynamics. Phys. Rev. D **13**, 191 (1976)
4. J.D. Bekenstein, Black-hole thermodynamics. Phys. Today **33**, 24–31 (1980)
5. D. Grumiller, R. McNees, Thermodynamics of black holes in two (and higher) dimensions. J. High Energy Phys. **2007**, 074 (2007)
6. R. Narayan, E. Quataert, Black holes up close. Nature **615**, 597–604 (2023)
7. C. Bambi, Astrophysical black holes: a compact pedagogical review. Ann. Phys. **530**, 1700430 (2018)
8. M.F. Wondrak, M. Bleicher, P. Nicolini, Black holes and high energy physics: from astrophysics to large extra dimensions. https://doi.org/10.48550/arXiv.1708.06763. [arXiv:1708.06763 [gr-qc]]

9. V.P. Frolov, Notes on nonsingular models of black holes. Phys. Rev. D **94**, 104056 (2016)
10. K. Schwarzschild, On the gravitational field of a mass point according to Einstein's theory (1999). arXiv preprint. arXiv:physics/9905030
11. G. Nordström, On the energy of the gravitation field in Einstein's theory. Koninklijke Nederlandse Akademie van Wetenschappen Proceedings Series B Physical Sciences **20**, 1238–1245 (1918)
12. A. Sean, Hayward, formation and evaporation of regular black holes. Phys. Rev. Lett. **96**, 031103 (2006). https://doi.org/10.1103/PhysRevLett.96.031103. arXiv:gr-qc/0506126
13. S. Guo, G.-R. Li, E.-W. Liang, Influence of accretion flow and magnetic charge on the observed shadows and rings of the Hayward black hole. Phys. Rev. D **105**, 023024 (2022)
14. S.A. Hayward, Inequalities relating area, energy, surface gravity, and charge of black holes. Phys. Rev. Lett. **81**, 4557 (1998)
15. S. Il'ich Kruglov, Remarks on nonsingular models of hayward and magnetized black hole with rational nonlinear electrodynamics. Gravit. Cosmol. **27**, 78–84 (2021)
16. Z. Song, H. Gong, H.-L. Li, F. Guoyang, L.-G. Zhu, W. Jian-Pin, Quasinormal modes and ringdown waveforms of a Frolov black hole. Commun. Theor. Phys. **76**, 105401 (2024). https://doi.org/10.1088/1572-9494/ad5717. arXiv:2406.04787 [gr-qc]
17. M.M. Gohain, K. Bhuyan, R. Borgohain, T. Gogoi, K. Bhuyan, P. Phukon, Frolov black hole surrounded by quintessence - I: Thermodynamics, geodesics and shadows. Nucl. Phys. B **1018**, 117073 (2025). https://doi.org/10.1016/j.nuclphysb.2025.117073. [arXiv:2412.06252 [gr-qc]]
18. F. John, Donoghue, general relativity as an effective field theory: the leading quantum corrections. Phys. Rev. D **50**, 3874–3888 (1994). https://doi.org/10.1103/PhysRevD.50.3874. arXiv:gr-qc/9405057
19. N. Sahan, E. Sucu, Y. Sucu, Quantum phase transitions of Dirac particles in a magnetized rotating curved background: Interplay of geometry, magnetization, and thermodynamics. Phys. Dark Univ. **49**, 102005 (2025). https://doi.org/10.1016/j.dark.2025.102005
20. T. Faulkner, A. Lewkowycz, J. Maldacena, Quantum corrections to holographic entanglement entropy. JHEP **11**, 074 (2013). https://doi.org/10.1007/JHEP11(2013)074. arXiv:1307.2892 [hep-th]
21. E. Sucu, İ. Sakalli, Quantum tunneling and Aschenbach effect in nonlinear Einstein–Power–Yang–Mills AdS black holes. Chin. Phys. C (2025). https://doi.org/10.1088/1674-1137/add8fe
22. J.F. Donoghue, Leading quantum correction to the Newtonian potential. Phys. Rev. Lett. **72**, 2996–2999 (1994). https://doi.org/10.1103/PhysRevLett.72.2996. arXiv:gr-qc/9310024
23. J. Alfaro, H.A. Morales-Tecotl, L.F. Urrutia, Quantum gravity corrections to neutrino propagation. Phys. Rev. Lett. **84**, 2318–2321 (2000). https://doi.org/10.1103/PhysRevLett.84.2318. arXiv:gr-qc/9909079
24. E. Sucu, I. Sakalli, B. Pourhassan, Quantum corrections in thermodynamics of black holes modified by nonlinear electrodynamics and their observational signatures. Int. J. Geom. Methods Mod. Phys. (2025). https://doi.org/10.1142/S0219887825502433?srsltid=AfmBOooJrA3ddqaCBZbmvNKDWMMyH7Tvw1gVTVRAREPfFjoEJLGnOipA
25. A. Sen, Logarithmic corrections to Schwarzschild and other non-extremal black hole entropy in different dimensions. JHEP **04**, 156 (2013). https://doi.org/10.1007/JHEP04(2013)156. arXiv:1205.0971 [hep-th]
26. I. Sakalli, M. Halilsoy, H. Pasaoglu, Entropy conservation of linear dilaton black holes in quantum corrected Hawking radiation. Int. J. Theor. Phys. **50**, 3212–3224 (2011)
27. E. Sucu, İ Sakallı, Dynamics of particles surrounding a stationary, spherically-symmetric black hole with nonlinear electrodynamics. Phys. Dark Universe **47**, 101771 (2025)
28. L. Junjie, W. Xin, Effects of two quantum correction parameters on chaotic dynamics of particles near renormalized group improved Schwarzschild black holes. Universe **10**, 277 (2024). https://doi.org/10.3390/universe10070277. arXiv:2406.18943 [gr-qc]
29. G. Gecim, Y. Sucu, Quantum gravity correction to hawking radiation of the 2 + 1-dimensional wormhole. Adv. High Energy Phys. **2020**, 7516789 (2020)
30. E. Sucu, I. Sakallı, Nonlinear electrodynamics effects on the geometry, thermodynamics, and quantum dynamics of (2+1)-dimensional black holes. Nucl. Phys. B **1015**, 116894 (2025). https://doi.org/10.1016/j.nuclphysb.2025.116894
31. G. Gecim, Y. Sucu, Quantum gravity effect on the Hawking radiation of spinning dilaton black hole. Eur. Phys. J. C **79**, 1–9 (2019)
32. E. Sucu, İ Sakallı, Astrophysical reality of black hole thermodynamics and dynamics: transformative influence of Hernquist dark matter distributions. Phys. Dark Universe **49**, 102051 (2025). https://doi.org/10.1016/j.dark.2025.102051
33. F. Ahmed, A. Al-Badawi, İ Sakallı, Some observable physical properties of Finslerian Hayward-like black hole with global monopole charge and quintessence field. Eur. Phys. J. C **85**, 668 (2025). https://doi.org/10.1140/epjc/s10052-025-14405-5
34. A. Al-Badawi, F. Ahmed, İ Sakallı, Dunkl black hole with phantom global monopoles: geodesic analysis, thermodynamics and shadow. Eur. Phys. J. C **85**, 660 (2025). https://doi.org/10.1140/epjc/s10052-025-14402-8
35. F. Ahmed, A. Al-Badawi, I. Sakallı, Ads black strings in a cosmic web: geodesics, shadows, and thermodynamics. Eur. Phys. J. C **85**, 554 (2025). https://doi.org/10.1140/epjc/s10052-025-14266-y. arXiv:2505.13833 [gr-qc]
36. F. Ahmed, A. Al-Badawi, İ Sakallı, Exploring geodesics, quantum fields and thermodynamics of Schwarzschild–AdS black hole with a global monopole in non-commutative geometry. Nucl. Phys. B **1017**, 116951 (2025). https://doi.org/10.1016/j.nuclphysb.2025.116951
37. F. Ahmed, A. Al-Badawi, İ Sakallı, Probing quantum gravity effects: geodesic structure and thermodynamics of deformed Schwarzschild AdS black holes surrounded by cosmic strings. Phys. Dark Universe **48**, 101925 (2025)
38. A. Lewis, A. Challinor, Weak gravitational lensing of the CMB. Phys. Rep. **429**, 1–65 (2006). https://doi.org/10.1016/j.physrep.2006.03.002. arXiv:astro-ph/0601594
39. N. Aghanim et al. (Planck), Planck 2018 results. VIII. Gravitational lensing. Astron. Astrophys. **641**, A8 (2020). https://doi.org/10.1051/0004-6361/201833886. arXiv:1807.06210 [astro-ph.CO]
40. K.S. Virbhadra, G.F.R. Ellis, Gravitational lensing by naked singularities. Phys. Rev. D **65**, 103004 (2002). https://doi.org/10.1103/PhysRevD.65.103004
41. H. Gursel, M. Mangut, E. Sucu, Thermodynamics of Einstein–Euler–Heisenberg black holes with thermal fluctuations and nonlinear electromagnetic fields. Class. Quantum Gravity (2025)
42. E. Sucu, İ Sakall, Exploring Lorentz-violating effects of Kalb–Ramond field on charged black hole thermodynamics and photon dynamics. Class. Quantum Grav. **42**, 135015 (2025)
43. F. Ahmed, A. Al-Badawi, I. Sakallı, Geodesics analysis, perturbations and deflection angle of photon ray in Finslerian Bardeen-like black hole with a GM surrounded by a quintessence field (2025). https://doi.org/10.1002/andp.202500087
44. F. Ahmed, A. Al-Badawi, İ Sakallı, Photon spheres, gravitational lensing/mirroring, and greybody radiation in deformed AdS–Schwarzschild black holes with phantom global monopole. Phys. Dark Universe **49**, 101988 (2025). https://doi.org/10.1016/j.dark.2025.101988. arXiv:2503.12092 [gr-qc]
45. F. Ahmed, İ. Sakallı, A. Al-Badawi, Gravitational lensing phenomena of Ellis–Bronnikov–Morris–Thorne wormhole with global monopole and cosmic string. Phys. Lett. B **864**,

139448 (2025). https://doi.org/10.1016/j.physletb.2025.139448. arXiv:2503.00082 [gr-qc]
46. M. Mangut, H. Gürsel, İ Sakallı, Lorentz-symmetry violation in charged black-hole thermodynamics and gravitational lensing: effects of the Kalb–Ramond field. Chin. Phys. C **49**, 065106 (2025). https://doi.org/10.1088/1674-1137/adbacf. arXiv:2504.02108 [gr-qc]
47. L. Stella, M. Vietri, Lense–Thirring precession and QPOs in low mass X-ray binaries. Astrophys. J. Lett. **492**, L59 (1998). https://doi.org/10.1086/311075. arXiv:astro-ph/9709085
48. V.M. Kaspi, A. Beloborodov, Magnetars. Annu. Rev. Astron. Astrophys. **55**, 261–301 (2017). https://doi.org/10.1146/annurev-astro-081915-023329. arXiv:1703.00068 [astro-ph.HE]
49. L. Stella, M. Vietri, S. Morsink, Correlations in the QPO frequencies of low mass X-ray binaries and the relativistic precession model. Astrophys. J. Lett. **524**, L63–L66 (1999). https://doi.org/10.1086/312291. arXiv:astro-ph/9907346
50. A. Ashraf, F. Javed, S.K. Maurya, P. Channuie, A. Cilli, E. Güdekli, Testing of rotating Einstein–Yang–Mills–Higgs black hole through QPOs. Phys. Dark Universe **48**, 101853 (2025). https://doi.org/10.1016/j.dark.2025.101853
51. T. Xamidov, U. Uktamov, S. Shaymatov, B. Ahmedov, Quasiperiodic oscillations around a Schwarzschild black hole surrounded by a Dehnen type dark matter halo. Phys. Dark Universe **47**, 101805 (2025). https://doi.org/10.1016/j.dark.2024.101805
52. H. Hoshimov, A. Davlataliev, F. Atamurotov, A. Abdujabbarov, A. Övgün, Particle dynamics and quasi-periodic oscillations in the Dyonic ModMax: constraint using quasars data. JHEAp **45**, 306–315 (2025). https://doi.org/10.1016/j.jheap.2024.12.012
53. C. Bambi, Probing the space-time geometry around black hole candidates with the resonance models for high-frequency QPOs and comparison with the continuum-fitting method. JCAP **09**, 014 (2012). https://doi.org/10.1088/1475-7516/2012/09/014. arXiv:1205.6348 [gr-qc]
54. E. Berti, V. Cardoso, A.O. Starinets, Quasinormal modes of black holes and black branes. Class. Quantum Gravity **26**, 163001 (2009). https://doi.org/10.1088/0264-9381/26/16/163001. arXiv:0905.2975 [gr-qc]
55. L. Barack et al., Black holes, gravitational waves and fundamental physics: a roadmap. Class. Quantum Gravity **36**, 143001 (2019). https://doi.org/10.1088/1361-6382/ab0587. arXiv:1806.05195 [gr-qc]
56. F. Scardigli, Generalized uncertainty principle in quantum gravity from micro-black hole gedanken experiment. Phys. Lett. B **452**, 39–44 (1999). https://doi.org/10.1016/S0370-2693(99)00167-7. arXiv:hep-th/9904025
57. S. Das, E.C. Vagenas, Universality of quantum gravity corrections. Phys. Rev. Lett. **101**, 221301 (2008). https://doi.org/10.1103/PhysRevLett.101.221301. arXiv:0810.5333 [hep-th]
58. E. Sucu, İ Sakallı, Quantum-corrected thermodynamics and plasma lensing of MOG black holes. Proc. R. Soc. A **481**, 20250251 (2025)
59. T. Zhu, J.-R. Ren, M.-F. Li, Influence of generalized and extended uncertainty principle on thermodynamics of FRW universe. Phys. Lett. B **674**, 204–209 (2009). https://doi.org/10.1016/j.physletb.2009.03.020. arXiv:0811.0212
60. A.J.M. Medved, E.C. Vagenas, When conceptual worlds collide: the GUP and the BH entropy. Phys. Rev. D **70**, 124021 (2004). https://doi.org/10.1103/PhysRevD.70.124021. arXiv:hep-th/0411022
61. C. Bambi, Testing black hole candidates with electromagnetic radiation. Rev. Mod. Phys. **89**, 025001 (2017). https://doi.org/10.1103/RevModPhys.89.025001. arXiv:1509.0388 [gr-qc]
62. J. Bardeen, Non-singular general relativistic gravitational collapse, in *Proceedings of the 5th International Conference on Gravitation and the Theory of Relativity* (1968), p. 87
63. K. Akiyama, A. Alberdi, W. Alef, K. Asada, R. Azulay, A-K. Baczko, D. Ball, M. Baloković, J.Barrett, D .Bintley, et al, First m87 event horizon telescope results. vi. the shadow and mass of the central black hole, The Astrophysical Journal Letters **875**(1), L6 ( 2019)
64. J.D. Bekenstein, Black holes and information theory. Contemp. Phys. **45**, 31–43 (2004)
65. G.W. Gibbons, M.C. Werner, Applications of the gauss-bonnet theorem to gravitational lensing. Class. Quant. Grav. **25**, 235009 (2008). https://doi.org/10.1088/0264-9381/25/23/235009. arXiv:0807.0854 [gr-qc]
66. K. Jusufi, A. Övgün, Gravitational lensing by rotating wormholes. Phys. Rev. D **97**, 024042 (2018). https://doi.org/10.1103/PhysRevD.97.024042. arXiv:1708.06725 [gr-qc] arXiv:1708.06725 [gr-qc]
67. M. Okyay, A. Övgün, Nonlinear electrodynamics effects on the black hole shadow, deflection angle, quasinormal modes and greybody factors. JCAP **01**, 009 (2022). https://doi.org/10.1088/1475-7516/2022/01/009. arXiv:2108.07766 [gr-qc]
68. S.U. Islam, R. Kumar, S.G. Ghosh, Gravitational lensing by black holes in the 4*d* einstein-gauss-bonnet gravity. JCAP **09**, 030 (2020). https://doi.org/10.1088/1475-7516/2020/09/030. arXiv:2004.01038 [gr-qc]
69. Erdem Sucu and Ali Övgün, The effect of quark–antiquark confinement on the deflection angle by the NED black hole, Phys. Dark Univ. **44**, 101446 ( 2024),https://doi.org/10.1016/j.dark.2024.101446 http://arxiv.org/abs/2403.07044 arXiv:2403.07044 [gr-qc]
70. Z. Li, G. Zhang, A. Övgün, Circular orbit of a particle and weak gravitational lensing. Phys. Rev. D **101**, 124058 (2020). https://doi.org/10.1103/PhysRevD.101.124058. arXiv:2006.13047 [gr-qc]
71. B. Puliçe, R.C. Pantig, A. Övgün, D. Demir, Constraints on charged symmergent black hole from shadow and lensing. Class. Quant. Grav. **40**, 195003 (2023). https://doi.org/10.1088/1361-6382/acf08c. arXiv:2308.08415 [gr-qc]
72. A. Övgün, I. Sakallı, Hawking radiation via gauss-bonnet theorem. Ann. Phys. **413**, 168071 (2020)
73. A.F. Ali, S. Das, E.C. Vagenas, Discreteness of space from the generalized uncertainty principle. Phys. Lett. B **678**, 497–499 (2009). https://doi.org/10.1016/j.physletb.2009.06.061. arXiv:0906.5396 [hep-th]
74. E. Sucu, İ Sakallı, Gup-reinforced hawking radiation in rotating linear dilaton black hole spacetime. Phys. Scripta **98**, 105201 (2023). https://doi.org/10.1088/1402-4896/acf2cf
75. S. Kanzi, I. Sakallı, Gup modified hawking radiation in bumblebee gravity. Nucl. Phys. B **946**, 114703 (2019)
76. G. Gecim, Y. Sucu, The gup effect on hawking radiation of the 2+1 dimensional black hole. Phys. Lett. B **773**, 391–394 (2017)
77. I. Cimidiker, M.P. Dabrowski, H. Gohar, Generalized uncertainty principle impact on nonextensive black hole thermodynamics. Class. Quant. Grav. **40**, 145001 (2023). https://doi.org/10.1088/1361-6382/acdb40. arXiv:2301.00609 [gr-qc]
78. M. Asghari, P. Pedram, K. Nozari, Harmonic oscillator with minimal length, minimal momentum, and maximal momentum uncertainties in susyqm framework. Phys. Lett. B **725**, 451–455 (2013). https://doi.org/10.1016/j.physletb.2013.07.030. arXiv:1307.7899 [hep-th]
79. G. Gecim, Y. Sucu, The gup effect on tunneling of massive vector bosons from the 2+1 dimensional black hole. Adv. High Energy Phys. **2018**, 7031767 (2018). https://doi.org/10.1155/2018/7031767. arXiv:1704.03537 [gr-qc]
80. B. Majumder, Effects of gup in quantum cosmological perfect fluid models. Phys. Lett. B **699**, 315–319 (2011). https://doi.org/10.1016/j.physletb.2011.04.030. arXiv:1104.3488 [gr-qc]

81. M. Dernek, C. Tekincay, G. Gecim, Y. Kucukakca, Y. Sucu, Hawking radiation of euler-heisenberg-ads black hole under the gup effect. The European Physical Journal Plus **138**, 369 (2023)
82. C. Rovelli, Black hole entropy from loop quantum gravity. Phys. Rev. Lett. **77**, 3288 (1996)
83. R. Bousso, The holographic principle for general backgrounds. Class. Quantum Gravity **17**, 997 (2000)
84. K. Jusufi, A. Övgün, A. Banerjee, Sakallı, gravitational lensing by wormholes supported by electromagnetic, scalar, and quantum effects. Eur. Phys. J. Plus **134**, 428 (2019). https://doi.org/10.1140/epjp/i2019-12792-9. arXiv:1802.07680 [gr-qc]
85. A. Övgün, Weak field deflection angle by regular black holes with cosmic strings using the gauss-bonnet theorem. Physical Review D **99**, 104075 (2019)
86. E. Sucu, İ Sakallı, Probing starobinsky-bel-robinson gravity: gravitational lensing, thermodynamics, and orbital dynamics. Nucl. Phys. B **1018**, 116982 (2025)
87. M.A. Troxel, M. Ishak, The intrinsic alignment of galaxies and its impact on weak gravitational lensing in an era of precision cosmology. Phys. Rept. **558**, 1–59 (2014). https://doi.org/10.1016/j.physrep.2014.11.001. arXiv:1407.6990 [astro-ph.CO]
88. A. Ashraf, A. Ditta, S.K. Abdelmalek Bouzenada, A.A.-E. Maurya, N.A.A. Suoliman, P. Channuie, Plasma lensing, epicyclic oscillations, particle collision, and thermal fluctuations around a short-hairy black hole. Phys. Dark Univ. **48**, 101836 (2025). https://doi.org/10.1016/j.dark.2025.101836
89. E. Elizalde, S. Nojiri, S.D. Odintsov, Late-time cosmology in (phantom) scalar-tensor theory: dark energy and the cosmic speed-up. Phys. Rev. D **70**, 043539 (2004). https://doi.org/10.1103/PhysRevD.70.043539. arXiv:hep-th/0405034
90. C.A.A. de Carvalho, H.M. Nussenzveig, Time delay. Phys. Rep. **364**, 83–174 (2002)
91. V. Bozza, L. Mancini, Time delay in black hole gravitational lensing as a distance estimator. Gen. Relativ. Gravit. **36**, 435–450 (2004)
92. K.S. Virbhadra, C.R. Keeton, Time delay and magnification centroid due to gravitational lensing by<? format?> black holes and naked singularities, physical review d–particles. Fields, Gravitation, and Cosmology **77**, 124014 (2008)
93. T. Hsieh, D.-S. Lee, C.-Y. Lin, Gravitational time delay effects by kerr and kerr-newman black holes in strong field limits. Physical Review D **104**, 104013 (2021)
94. C.-K. Qiao, S. Ping, Time delay of light in the gravitational lensing of supermassive black holes in dark matter halos. The European Physical Journal C **84**, 1032 (2024)
95. G. Wang, SATDI: Simulation and Analysis for Time-Delay Interferometry, (2024), http://arxiv.org/abs/2403.01726 arXiv:2403.01726 [gr-qc]
96. D. Psaltis, Testing general relativity with the event horizon telescope. Gen. Relativ. Gravit. **51**, 137 (2019)
97. Nicholas David Birrell and Paul Charles William Davies, Quantum fields in curved space, (1984)
98. R.M Wald, *Quantum field theory in curved spacetime and black hole thermodynamics* ( University of Chicago press, 1994)
99. C. Bambi, D. Malafarina, L. Modesto, Non-singular quantum-inspired gravitational collapse. Phys. Rev. D **88**, 044009 (2013). https://doi.org/10.1103/PhysRevD.88.044009. arXiv:1305.4790 [gr-qc]
100. A. Simpson, M. Visser, Black-bounce to traversable wormhole. JCAP **02**, 042 (2019). https://doi.org/10.1088/1475-7516/2019/02/042. arXiv:1812.07114 [gr-qc]
101. P. Nicolini, A. Smailagic, E. Spallucci, Noncommutative geometry inspired schwarzschild black hole. Phys. Lett. B **632**, 547–551 (2006). https://doi.org/10.1016/j.physletb.2005.11.004. arXiv:gr-qc/0510112
102. A. Smailagic, E. Spallucci, Feynman path integral on the non-commutative plane. J. Phys. A **36**, L467 (2003). https://doi.org/10.1088/0305-4470/36/33/101. arXiv:hep-th/0307217
103. J.D. Bekenstein, Black holes and entropy. Physical Review D **7**, 2333 (1973)
104. Abdel Nasser Tawfik and Abdel Magied Diab, Generalized uncertainty principle and recent cosmic inflation observations. Electron. J. Theor. Phys. **12**, 9–30 (2015). arXiv:1410.7966 [gr-qc]
105. İ Sakallı, S. Kanzi, Physical properties of brane-world black hole solutions via a confining potential. Annals Phys. **439**, 168803 (2022). https://doi.org/10.1016/j.aop.2022.168803. arXiv:2201.00537 [hep-th]
106. K. Srinivasan, T. Padmanabhan, Particle production and complex path analysis. Physical Review D **60**, 024007 (1999)
107. W. Javed, R. Babar, A. Övgün, Hawking radiation from cubic and quartic black holes via tunneling of gup corrected scalar and fermion particles. Mod. Phys. Lett. A **34**, 1950057 (2019)
108. M.K. Parikh, F. Wilczek, Hawking radiation as tunneling. Phys. Rev. Lett. **85**, 5042 (2000)
109. M. Angheben, M. Nadalini, L. Vanzo, S. Zerbini, Hawking radiation as tunneling for extremal and rotatingblack holes. J. High Energy Phys. **2005**, 014 (2005)
110. T. Zhu, J.-R. Ren, M.-F. Li, Influence of generalized and extended uncertainty principle on thermodynamics of frw universe. Phys. Lett. B **674**, 204–209 (2009)
111. D.J. Gross, P.F. Mende, String theory beyond the planck scale. Nucl. Phys. B **303**, 407–454 (1988)
112. D. Amati, M. Ciafaloni, G. Veneziano, Can spacetime be probed below the string size? Phys. Lett. B **216**, 41–47 (1989)
113. A. Ashtekar, J. Lewandowski, Background independent quantum gravity: a status report. Class. Quantum Gravity **21**, R53 (2004)
114. C. Rovelli, Loop quantum gravity. Living Rev. Relativ. **11**, 5 (2008)
115. G. Amelino-Camelia, Relativity in spacetimes with short-distance structure governed by an observer-independent (planckian) length scale. International Journal of Modern Physics D **11**, 35–59 (2002)
116. J. Kowalski-Glikman, Observer-independent quantum of mass. Phys. Lett. A **286**, 391–394 (2001)
117. A. Kempf, G. Mangano, And robert b mann, hilbert space representation of the minimal length uncertainty relation. Physical Review D **52**, 1108 (1995)
118. L.J. Garay, Quantum gravity and minimum length. Int. J. Mod. Phys. A **10**, 145–165 (1995)
119. M.C. Werner, Gravitational lensing in the kerr-randers optical geometry. Gen. Relativ. Gravit. **44**, 3047–3057 (2012)
120. A. Ishihara, Y. Suzuki, T. Ono, T. Kitamura, H. Asada, Gravitational bending angle of light for finite distance and the gauss-bonnet theorem. Physical Review D **94**, 084015 (2016)
121. E. Sucu ,İ. Sakallı, Astrophysical reality of black hole thermodynamics and dynamics: Transformative influence of hernquist dark matter distributions, Physics of the Dark Universe , 102051 (2025f)
122. C.Bambi, *Black holes: a laboratory for testing strong gravity*, Vol. 10 ( Springer, 2017)
123. H. Hoshimov, O. Yunusov, F. Atamurotov, M. Jamil, A. Abdujabbarov, Particle dynamics and quasi-periodic oscillations in the gup-modified schwarzschild spacetime: constraint using micro-quasars data. Astropart. Phys. **165**, 103056 (2025)
124. A. Edery, M.B. Paranjape, Classical tests for weyl gravity: deflection of light and time delay. Physical Review D **58**, 024011 (1998)
125. S. Gao, R.M. Wald, Theorems on gravitational time delay and related issues. Class. Quantum Gravity **17**, 4999 (2000)
126. F.B. Estabrook, Massimo tinto, and jw armstrong, time-delay analysis of lisa gravitational wave data: elimination of spacecraft motion effects. Physical Review D **62**, 042002 (2000)

127. R.J. Adler, P. Chen, D.I. Santiago, The generalized uncertainty principle and black hole remnants. Gen. Relativ. Gravit. **33**, 2101–2108 (2001)
128. L. Zhao, M. Tang, X. Zhaoyi, The lensing effect of quantum-corrected black hole and parameter constraints from eht observations. The European Physical Journal C **84**, 971 (2024)
129. X-J. Gao, Strong gravitational lensing of regular black holes in asymptotically safe gravity, arXiv preprint arXiv:2411.09513 ( 2024)
130. V. Husain, R.B. Mann, Thermodynamics and phases in quantum gravity. Class. Quantum Gravity **26**, 075010 (2009)
131. Z.W. Feng, H.L. Li, X.T. Zu, S.Z. Yang, Quantum corrections to the thermodynamics of schwarzschild-tangherlini black hole and the generalized uncertainty principle. The European Physical Journal C **76**, 212 (2016)
132. R. López-Coto, Michele doro. A De Angelis, M Mariotti, and James Patrick Harding, Prospects for the observation of primordial black hole evaporation with the southern wide field of view gamma-ray observatory, Journal of Cosmology and Astroparticle Physics **2021**, 040 (2021)
133. N.U.Molla, A. Ali, U. Debnath, Observational signatures of modified bardeen black hole: shadow and strong gravitational lensing, arXiv preprint arXiv:2307.11798 ( 2023)
134. E. Bagui, S. Clesse, V. De Luca, J.M. Ezquiaga, G. Franciolini, J. García-Bellido, C. Joana, R.K. Jain, S. Kuroyanagi, I. Musco et al., Primordial black holes and their gravitational-wave signatures. Living Rev. Relativ. **28**, 1 (2025)
135. P.V.P. Cunha, C.A.R. Herdeiro, Shadows and strong gravitational lensing: a brief review. Gen. Relativ. Gravit. **50**, 1–27 (2018)
136. Niyaz Uddin Molla, Himanshu chaudhary. G Mustafa, Ujjal Debnath, and SK Maurya, Strong gravitational lensing, quasi-periodic oscillations and constraints from eht observations for quantum-improved charged black hole, The European Physical Journal C **84**, 390 (2024)
137. A. Strominger, C. Vafa, Microscopic origin of the bekenstein-hawking entropy. Phys. Lett. B **379**, 99–104 (1996)
138. R. Banerjee, Bibhas ranjan majhi, and saurav samanta, noncommutative black hole thermodynamics, physical review d–particles. Fields, Gravitation, and Cosmology **77**, 124035 (2008)
139. A. Burkert, The structure of dark matter halos in dwarf galaxies. Astrophys. J. **447**, L25 (1995)
140. I.V. Igumenshchev, M.A. Abramowicz, Two-dimensional models of hydrodynamical accretion flows into black holes. Astrophys. J. Suppl. Ser. **130**, 463 (2000)
141. R.F. Coker, F. Melia, Hydrodynamical accretion onto sagittarius a* from distributed point sources. Astrophys. J. **488**, L149 (1997)